Engineered Science
DOI: https://dx.doi.org/10.30919/es1149

Preparing High-Quality Monolithic Carbon Nanotubes Reinforced Silica Aerogel Composites Based on a Vacuum Freeze-Drying Method

Zhenting Zhu,[1, 2,#] Huangshuai Zhang,[1, 2,#] Yu Ma,[1,*] Zihao Yang[1, 2] Zhe Chen[1] and Hang Zhang[1,*]

Abstract

In this study, using tert-butanol/water co-solvent as the freeze-drying solvent, we successfully prepared high-quality monolithic carbon nanotubes (CNTs) reinforced silica aerogel composites. The effects of CNTs on the pore structures, thermal performance and mechanical properties of the CNTs/silica aerogel composites were investigated. Generally, when the CNTs content is below 4 wt.%, the CNTs are uniformly distributed in the silica aerogel matrix due to the effective ultrasonic dispersion process. In addition, the CNTs form a good interface combination with the aerogel skeleton through the condensation of hydroxyl groups. Correspondingly, the pore structures and thermal conductivity of the composites were only slightly influenced, while the mechanical properties were greatly improved from 401.4 kPa to 658.6 kPa. However, due to the agglomeration and sedimentation of CNTs, the pore structure and the thermal insulation properties of the composite began to deteriorate when its content reached 6 wt.%, and its enhancing effect on mechanical properties also deteriorates significantly when the CNTs content reached 8 wt.%. This study provides a cost-effective process for preparing high-quality bulk CNTs/silica aerogel composites, which is beneficial for their future practical applications and commercialization.

Keywords: Silica aerogels; Carbon nanotubes; Tert-butanol/water co-solvent; Vacuum freeze-drying; Thermal and mechanical properties.
Received: 14 November 2023; Revised: 07 March 2024; Accepted: 24 March 2024.
Article type: Research article.

1. Introduction

As one kind of typical monolithic mesoporous material, silica aerogels have high porosity (80-99.8%), low bulk density (~0.003 g/cm^3), large specific surface area (SSA, 500-1200 m^2/g), low thermal conductivity (~0.005-0.040 W/(m·K)) and ultralow dielectric constant (k=1.0-2.0).[1-3] Due to these attractive characteristics, silica aerogels show great application potential in the fields of adsorbents, catalyst substrates, thermal insulators, acoustic insulation materials, dielectric materials, *etc*., and have attracted extensive attention.[4-8] Despite their attractive characteristics, the nanoporous structure also results in the inherent brittleness of silica aerogels, which makes their processing and handling extremely difficult and severely limits their application.[9,10]

In order to overcome the intrinsic drawbacks of silica aerogels and broaden their applicability, many attempts have been made during the past decades, such as the conventional introducing reinforcement fibers into aerogel matrix,[11,12] generating linear polymer structures by mixing the precursors,[13,14] and the novel assembling flexible silica nanofibers with a high length-to-diameter ratio into a highly continuous interwoven cellular structure.[15-17] The practical application of the latter two strategies is greatly constrained by the soaring cost, while the former one with a relative low cost has been the focus of relevant research. Considering the intrinsic features of fibers (strength, flexibility, length, diameter, length-to-diameter ratio, thermal stability, *etc*.) determine the final mechanical and thermal properties of silica aerogel composites, the accurate selection of reinforcement fibers (including organic, inorganic, and carbon fibers) is of great importance.[18-20] As a typical carbon fiber, carbon nanotubes (CNTs) are one of the strongest and stiffest materials due to the covalent bonding between individual carbon atoms, which makes them one of the most ideal

[1] *Institute of Engineering Thermophysics, Chinese Academy of Sciences, Beijing 100190, China.*
[2] *School of Energy Power and Mechanical Engineering, North China Electric Power University, Beijing 102206, China.*
[#] *These two authors contributed equally to this work.*
**Email:* mhemark@hotmail.com (Y. Ma); zhanghang@iet.cn (H. Zhang)

candidates for reinforcing silica aerogels.[21] Accordingly, considerable relevant research has been carried out during the past decades.[22-24] For example, Chernov *et al*.[23] has successfully synthesized silica aerogels doped with a maximum of 0.8 wt.% CNTs, which has a bulk density of 0.25 g/cm^{-3} and an average pore size of 3-20 nm. Similarly, Bargozin *et al*.[24] reinforced the silica aerogel matrix with 0.05 g CNTs, and the prepared composite had an SSA of 802 m^2.g^{-1}, a bulk density of 0.23 g/cm^{-3} and an average pore size of 2.5 nm.

As a critical step in the synthesis process, the drying procedure determines the final thermal and mechanical performance of CNTs reinforced silica aerogel composites (hereafter referred to as CNTs/silica aerogel composites).[2,21] Currently, most CNTs/silica aerogel composites are prepared by conventional supercritical drying (SCD) or ambient pressure drying (APD) methods.[25-28] For instance, Song *et al*.[25] and Duque *et al*.[26] have synthesized the CNTs/silica aerogel composites via a CO_2 SCD process, while Sun *et al*.[27] and Bangi *et al*.[28] have successfully prepared them using the APD method. However, the SCD process is insecure and energy-intensive for it needs to be conducted in high pressure, which severely limits its large-scale application.[29,30] In the meantime, the APD method is time-consuming and not environmentally friendly considering it involves the mass use of hazardous solvents to reduce serious pore collapse.[2,31] Vacuum freeze-drying (VFD) technique is another promising drying method for aerogels, which has the advantages of high efficiency, low cost, and high safety, and has shown its superiority in the preparation of cellulose,[32, 33] organic[34,35] and carbon-based aerogels.[36,37] Unfortunately, previous studies have shown that silica aerogels or CNTs/silica aerogel composites tend to break into fragments or powders during the freeze-drying process.[38,39] Hence, it is generally believed that they cannot be obtained by the VFD method.

In this study, TEOS and CNTs in different mass ratios were chosen to prepare the CNTs/silica alcogel via the sol-gel method. Then, high-quality monolithic CNTs/silica aerogel composites were successfully prepared through the VFD process using tert-butanol (TBA)/water co-solvent as the freeze-drying solvent. Subsequently, a high-efficiency chemical vapor deposition hydrophobic modification (CVDHM) process was carried out on the silica aerogels. The prepared bulk composites are totally crack-free and superhydrophobic, and show a series of excellent characteristics such as high SSAs, improved mechanical properties and low thermal conductivity. This study demonstrates that it is feasible to prepare high-quality bulk CNTs/silica aerogel composites via a VFD process and provides a cost-effective way to obtain them.

2. Experimental

2.1 Materials

The materials used in this study mainly include: Tetraethylorthosilicate (TEOS, GC), Absolute ethyl alcohol (EtOH, AR), Distilled water (H_2O), Glacial acetic acid (HOAc), N, N-Dimethylformamide (DMF, AR), Ammonia solution (AR), Tert-butyl alcohol (TBA, GC), Diethoxydimethylsilane (DMDES, 98%), Ammonium acetate (AR), Hydroxylated multiwalled carbon nanotubes (MWCNTs). The diameter of MWCNTs is about 40 nm, the length is 10-40 μm, and the purity is higher than 90%. All the chemical reagents were purchased from Shanghai Aladdin Biochemical Technology Co., Ltd.

2.2 Preparation procedure

2.2.1 Synthesis of CNTs/silica alcogel

TEOS, EtOH, H_2O and HOAc were mixed in specific proportions and magnetically stirred for 30 min. A certain amount of DMF was added into the mixed solution, stirred for 30 min, and maintained at 45 ℃ in water bath for 12 h to ensure sufficient hydrolysis under acidic condition. The molar ratio of TEOS, EtOH, H_2O, HOAc and DMF was kept constant at 1:10:3:0.3:0.25. Subsequently, a 2 mol/L ammonia solution was added dropwise to the silica sol under magnetic stirring until the pH rose to ~7. Then, hydroxylated MWCNTs with a mass ratio of 0 wt.%, 2 wt.%, 4 wt.%, 6 wt.%, 8 wt.% in the final silica aerogel composites (the adding amounts of MWCNTs were determined by measuring the mass ratio of prepared pure silica aerogel to silica sol) were added into the silica sol respectively, and subjected to ultrasonic dispersion for 40 min to make them fully and evenly mixed in the silica sol. Afterwards, the silica sol with uniformly distributed MWCNTs was poured into the mold and maintained at room temperature (RT) to gel.

2.2.2 Aging and solvent replacement

The as-prepared CNTs/silica alcogel samples were first aged at 45 ℃ for 6 h, and then completely immersed in ethanol at 45 ℃ for 36 h to strengthen the skeleton networks. Then, the alcogel samples were subjected to solvent replacement for 12 h, 12 h, 18 h and 24 h successively using 4~5 times the alcogel volume of TBA/H_2O mixture, by which the original aging solution has been completely replaced with the TBA/H_2O co-solvent containing 20 wt.% deionized water.

2.2.3 VFD and CVDHM

The CNTs/silica alcogel samples were first pre-frozen at -50 ℃ for 2 h. Then, they were freeze-dried in a vacuum freeze drier for 48 h to obtain dried CNTs/silica aerogel composites, during which the freeze-drying temperature was gradually increased from -50 ℃ to 50 ℃. The freeze-dried CNTs/silica aerogel composites, the hydrophobic modifier (DMDES) and the corresponding reaction auxiliary agent (ammonium acetate) were placed in an airtight container to carry out hydrophobic modification at 75 ℃ for 4 h. Afterwards, the residual modifier and reaction auxiliary agent were removed by vacuum treatment and the hydrophobic modified CNTs/silica aerogel composites were acquired. The mass ratio of CNTs/silica aerogel composite, DMDES and ammonium acetate is 1: 0.4:

0.15. The experimental procedure for the preparation is illustrated in Fig. 1.

2.3 Characterization

The bulk densities of the CNTs/silica aerogel composites were obtained from the mass (measured by a precision balance, Mettler Toledo, MS304TS/02) to volume (determined by measuring dimensions) ratio. The SSA and pore size distribution (PSD) of the composites were analyzed by nitrogen gas absorption and desorption method (JWGB SCI. & TECH, JW-TB200, China). Brunauer-Emmett-Teller (BET) and the Barrett-Joyner-Halenda (BJH) method was used for SSAs and PSD estimation, respectively. The adsorbate, degassing temperature and degassing time were N_2, 200 ℃ and 3 h, accordingly. The hydrophobicity was determined by measuring the contact angle θ of the water droplets dropped on the flat surface of CNTs/silica aerogel composites using a contact angle goniometer (Dynetech, SDC-200SH, China). The Fourier transform infrared spectroscopy (FTIR, Thermo Scientific, Nicolet iS50, USA) was employed to determine the chemical bonding state of silica aerogels. The CNTs/silica aerogel samples were ground into refined powders in advance, mixed with KBr, and pressed to form sample pellets. The microstructure of the CNTs/silica aerogel composites was observed using a scanning electron microscopy (SEM, Hitachi, S-4800, Japan). The CNTs/silica aerogel samples were crushed into fragments, dried in a vacuum chamber, and covered with a gold layer. The skeleton network structure inside the secondary particles was characterized by a transmission electron microscopy (TEM, JEOL, JEM-2100F, Japan) operated at 200 kV. The CNTs/silica aerogel samples were ground into powders and uniformly dispersed in ethanol using an ultrasonic bath. A drop of the suspension was deposited on a TEM holder and dried at 80 ℃ for 1 h to obtain the TEM specimens.

2.4 Thermal and mechanical testing

The room temperature thermal conductivity of the CNTs/silica aerogel composites was measured by a thermal conductivity instrument (Xiaxi Technology, TC 3000E, China) through a hot wire method. The thermal stability of them was tested in air atmosphere using a thermos gravimetric and differential thermal analyzer (TG-DTA, NANJING DAZHAN, DZ-TGA105, China) from room temperature to 850 ℃ with a heating rate of 10 ℃/min. TG-DTA was used to determine the oxidation temperature of the -CH_3 groups contained in the CNTs/silica aerogel composites, i.e., the temperature at which the aerogel composites retain their hydrophobicity. The compressive properties of the CNTs/silica aerogel composites were tested by a mechanical testing machine (QIYATEST, QY-1102, China) at a loading rate of 1 mm/min.

3. Results and discussion

3.1 Appearance and microstructure characterization

Figure 2 shows the optical images of the as-prepared CNTs/silica aerogel composites. High-quality monolithic CNTs/silica aerogel samples reinforced with 0 wt.%, 2 wt.%, 4 wt.%, 6 wt.% and 8 wt.% of CNTs (Figs. 2a-e, hereafter referred to as CNT-0, CNT-2, CNT-4, CNT-6, and CNT-8, accordingly) have been synthesized successfully. All the CNTs/silica aerogel samples are opaque, while their color gradually changes from opalescent to black with increasing CNTs addition. The surfaces of all the CNTs/silica aerogel samples are very smooth and no cracks are observed, which indicates no serious deformation or cracking occurred in the VFD procedure. Hence, it is proved that the VFD technique used in this study is effective and practical for extracting the liquid of CNTs/silica aerogel composites prepared by sol-gel transition without destroying the gel skeleton. In addition, there are river-like patterns on the upper surface of the aerogel samples, which should be caused by the freeze-drying solvent left there during the pre-freezing process.

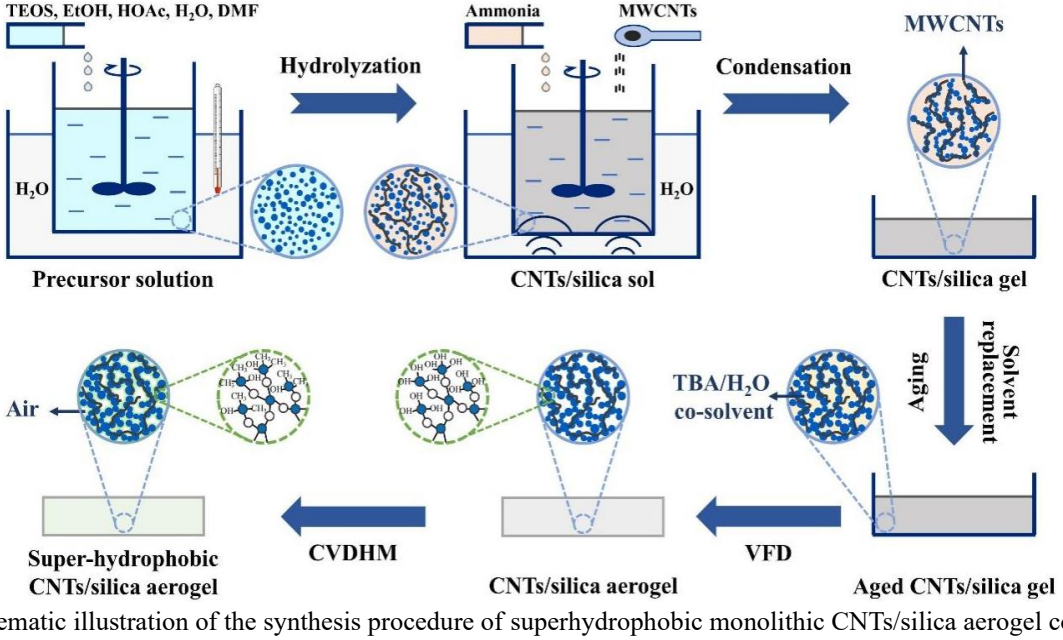

Fig. 1 Schematic illustration of the synthesis procedure of superhydrophobic monolithic CNTs/silica aerogel composites.

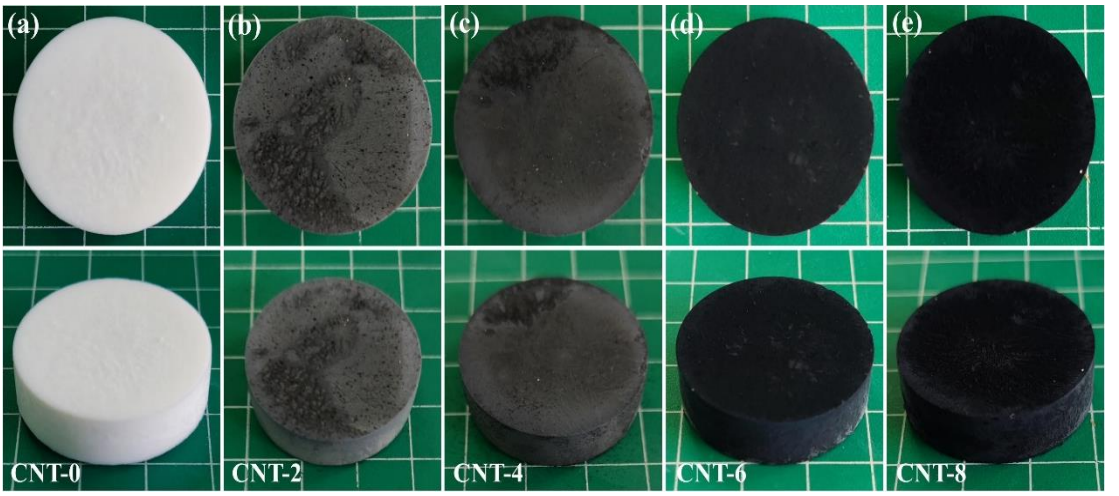

Fig. 2 Photograph of the as-prepared CNTs/silica aerogel samples reinforced with (a-e) 0 wt.%, 2 wt.%, 4 wt.%, 6 wt.% and 8 wt.% of CNTs. The grid spacing in the background is 10 mm.

Figure 3 presents the representative SEM images of the CNTs/silica aerogel composites. Their matrix presents a framework of interconnected pearl-like secondary particle clusters (Fig. 3a), which is composed of fine primary particles. According to the TEM image (Fig. 3b), it can be clearly observed that the aggregation of nanoscale primary particles leads to the formation of well-developed mesoporous structures inside the secondary particle clusters. Hence, the matrix of the as-prepared CNTs/silica aerogel composites exhibits a typical microstructure of silica aerogels, suggesting that the freeze-drying process did not cause significant crushing damage to the pore structure. As is well-known, the destruction of the nanoporous structure during freezing-drying is mainly caused by the growth of crystals inside the alcogel.[2,40] In this study, TBA/H_2O co-solvent was chosen as the freeze-drying solvent, which has a small volume change rate and forms fine needle-like ice crystals under freezing.[41] In this way, the extrusion damage of the formed ice crystals to the finely reticulated structures was minimized, resulting in high-quality monolithic CNTs/silica aerogel composites.

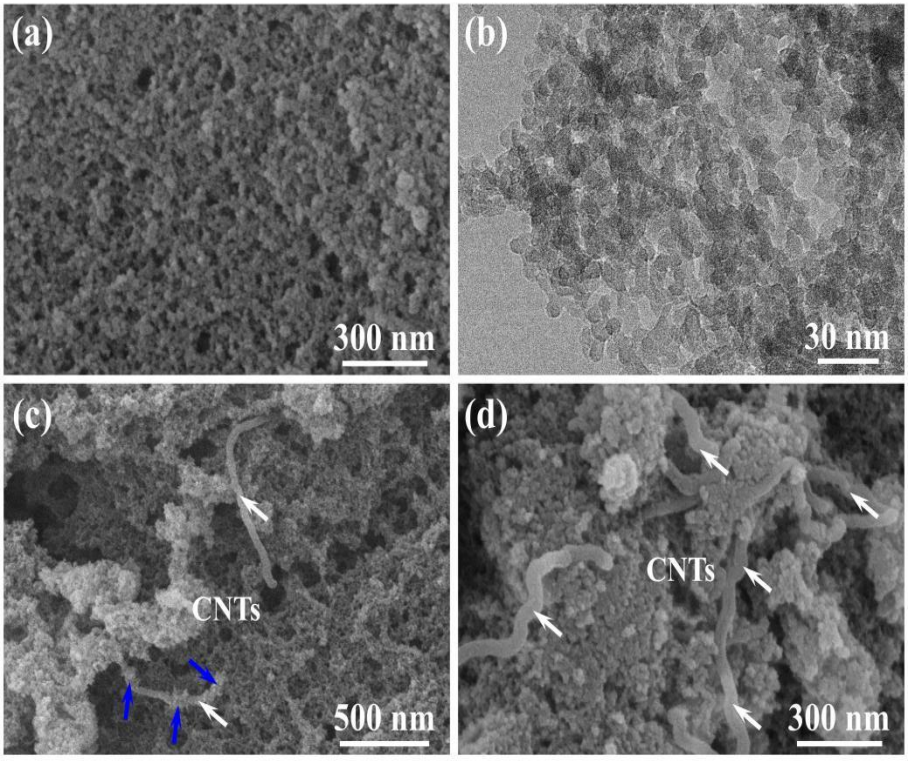

Fig. 3 (a) SEM image of the matrix of the CNTs/silica aerogel composites; (b) TEM image reveals the mesoporous skeleton structure inside the secondary particle clusters composed of nanoscale primary silica particles; (c) SEM image presents the CNT that distributed inside the silica aerogel matrix, the blue arrows point to the part of the CNT tightly wrapped by secondary particle clusters, and the white arrows point to the exposed part of CNT; (d) SEM image shows the CNT clusters found in the CNTs/silica aerogel composites (6 wt.%).

Figure 3c shows the CNTs distributed in the silica aerogel matrix. Some of the CNTs are tightly wrapped by the secondary particle clusters, indicating that the hydroxylated CNTs are well bonded with the matrix.[28] For samples with CNTs content below 4 wt.%, no agglomeration or entanglement of CNTs was found, which indicates that ultrasonic dispersion can make CNTs well dispersed in silica sol. However, ultrasonic dispersion becomes difficult to completely overcome the Van der Waals force between CNTs with the increasing CNTs content. As a result, some CNTs began to agglomerate and entangle with each other in the aerogel matrix (Fig. 3d), which shall have a negative impact on the thermal insulation and mechanical properties of the composites.

3.2 Densities, SSAs and pore structures

As shown in Fig. 4, the density of the CNTs/silica aerogel composite increases slightly with the increase of CNTs mass fraction. Fig. 5a gives the N_2 adsorption-desorption isotherms of the silica aerogels reinforced with different mass fractions of CNTs. All samples exhibit typical IV isotherms with H1 type hysteresis loops, the hysteresis loop is wide and the saturated adsorption platform is short, indicating that they are typical mesoporous materials with highly similar nonuniform and irregular pore structures.[39,42] The PSDs of CNTs/silica aerogel composites measured by BJH method are presented in Fig. 5b. It is evident that the samples exhibit a well-developed mesoporous distribution in the range of ~2-30 nm, with the peak occurring at about 10-20 nm. In addition, the PSD curves of the samples with CNTs content between 0-4 wt.% basically overlap, indicating the introduction of CNTs has limited effect on the pore structure and PSDs of the aerogel matrix. This is because the ultrasonic dispersion method can uniformly disperse CNTs in the matrix and avoid agglomeration under the appropriate amount of carbon nanotubes added, so the pore structure is less affected. However, when the CNTs content increased to 6 wt.%, the peak value of the PSD curves decreases, the peak becomes wider and begins to shift to the direction of larger pore size, and this trend becomes more pronounced when the content increases to 8 wt.%. This should be because when the CNTs content is high, their agglomeration and winding in the matrix gradually become serious (Fig. 3d), which reduces the homogeneity of the pore structure of the samples.

3.3 Hydrophobic property

The FTIR spectra of the CNTs/silica aerogel composites are given in Fig. 6 to reveal the information of chemical bonds. Comparing with the silica aerogel matrix, the addition of CNTs did not cause discernible changes in the infrared spectrum, and the peak value of group vibration was only slightly changed. Therefore, the addition of CNTs had no obvious effect on the group type of the CNTs/silica aerogel composites. In addition, for the hydrophobic modified samples, the adsorption peaks near ~850 cm^{-1} and 1260 cm^{-1} were caused by the stretching vibration of Si-C bond, while the weak peaks at 2970 cm^{-1} derived from the stretching vibration of -CH groups.[43,44] These results showed that the $-CH_3$ hydrophobic groups have been successfully introduced into the aerogel skeleton by CVDHM. Accordingly, as shown in Fig. 7, the CNTs/silica aerogel composite samples show superhydrophobicity with a contact angle of 152.4° for the silica aerogel matrix and above 151.4° for the CNTs/silica aerogel composites at a low modifier/aerogel mass ratio of 0.4.

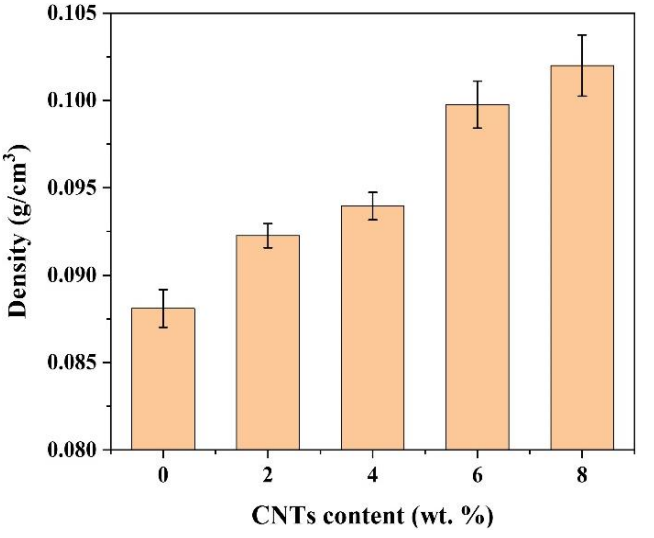

Fig. 4 The bulk densities of the CNTs/silica aerogel composites reinforced with different CNTs contents.

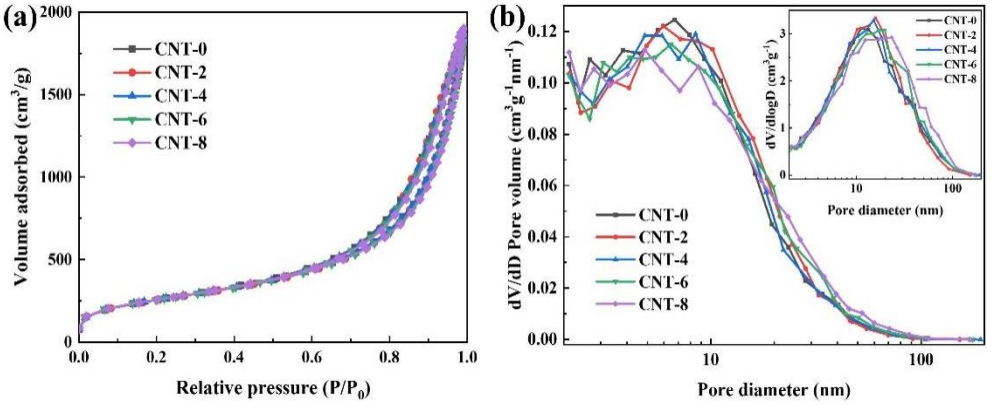

Fig. 5 N_2 adsorption-desorption isotherms and (b) dV/dlogD pore size distribution measured by BJH method of the CNTs/silica aerogel composites.

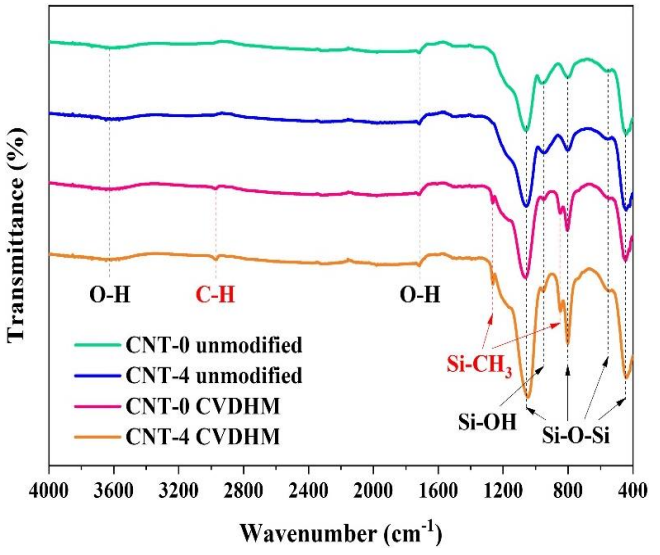

Fig. 6 FTIR spectra of the CNTs/silica aerogel composites with and without CVDHM process.

3.4 Thermal and mechanical properties

Figure 8 shows the thermal conductivity of the silica aerogel composites reinforced with different CNTs contents. When the mass fraction of CNTs is in the range of 2-4 wt.%, the thermal conductivity of composite aerogel changed little compared to pure aerogel (around 0.027 W/(m·K)), indicating that the CNTs achieved good dispersion in the aerogel matrix without forming obvious bridging to increase the heat conduction path. The sample reinforced with 2 wt.% CNTs has the lowest thermal conductivity, which should be attributed to the optimized pore structure caused by the introduced CNTs.[45,46] However, when the mass fraction of CNTs increased above 6 wt.%, the thermal conductivity of the composite increased with the increase of CNTs content, which should be attributed to the local agglomeration of CNTs in the aerogel matrix. The agglomerated and entangled CNTs bridged each other in the aerogel matrix, which increased the solid heat conduction path and thus the increased thermal conductivity of the composite.[47,48]

Figure 9 presents the thermal stability of the original and hydrophobically modified CNTs/silica aerogel composites. According to the TG-DSC results obtained in air atmosphere (Fig. 9a), the entire process for the unmodified CNT-0 sample can be divided into two stages. In stage I (RT-200 °C), the sample lost about 8.33% of its weight at a fast rate, which is due to the evaporation of residual solvent and moisture absorbed from the air.[49,50] The relatively low weight loss of ~3.53% in stage II (200-850 °C) is mainly caused by the condensation of Si-OH groups on the skeleton surface.[51] Meanwhile, the whole process for the CNT-0 sample treated by CVDHM can be divided into three stages (Fig. 9b). Its weight loss in stage I (RT-247 °C) is about 2.15%, which is significantly lower than the unmodified sample considering less moisture was adsorbed from the air due to the strong hydrophobicity. Stage II (247-600 °C) shows a weight loss of ~4.68%, which is mainly attributed to the thermal decomposition of $Si-CH_3$ groups.[51,52] According to the corresponding DSC curve, there is an obvious exothermic phenomenon at this stage from 247 °C, and the exothermic peak appears at about 269 °C, which means that the thermal stability temperature of the hydrophobically modified sample is about 247 °C. In stage III, the sample experienced a weight loss of 0.66% at a slow rate due to the condensation of Si-OH groups remaining in the aerogel skeleton.[38,50] The TG-DSC curves of the CNT-4 samples before and after hydrophobic modification are given in Figs. 9c and d. The thermal decomposition characteristics of CNT-0 and CNT-4 samples are basically the same below 600 °C, while the weight loss of the latter is much higher from 600 °C to 850 °C due to the thermal decomposition of CNTs.[53] In general, CVDHM treatment significantly improved the hydrophobic properties of the CNTs/silica aerogel composites. Since the introduced CNT begins to decompose above 600 °C, it has little effect on the thermal decomposition characteristics below 600 °C (the thermal stability temperature of the hydrophobically modified sample slightly improved to 257 °C).

Figure 10 shows the compressive properties of the as-

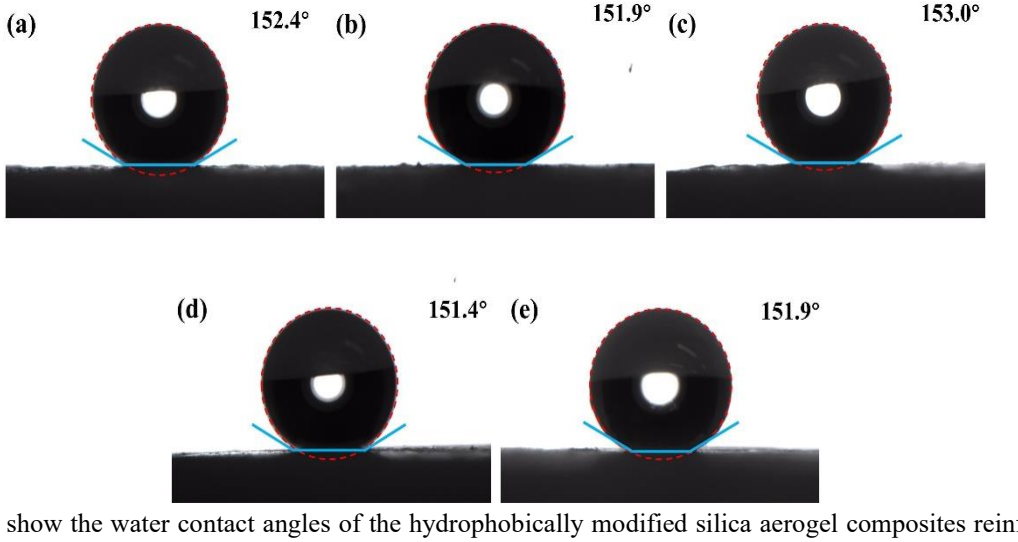

Fig. 7 Photographs show the water contact angles of the hydrophobically modified silica aerogel composites reinforced with (a) 0 wt.%, (b) 2 wt.%, (c) 4 wt.%, (d) 6 wt.%, and (e) 8 wt.% of CNTs.

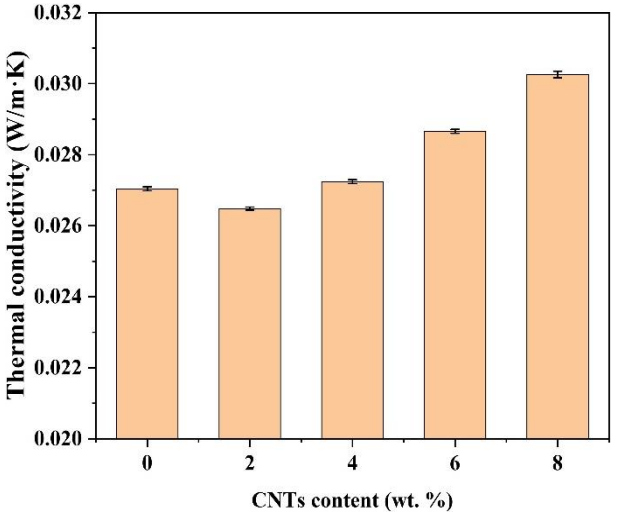

Fig. 8 Thermal conductivity of the CNTs/silica aerogel composites.

prepared CNTs/silica aerogel composites. Obviously, the addition of CNTs effectively improved the mechanical performance (the ability to resist brittle failure under increasing load and mechanical properties such as Young's modulus) of the composites, and the improvement range increased with the increase of the addition amount. As the strain gradually increased to more than 10%, the CNTs/silica aerogel samples began to show brittle failure. In this process, the stress growth rate of pure silica aerogel decreased sharply and showed obvious yield process. However, the silica aerogel composites strengthened by CNTs did not show typical yield phenomenon, the slope of the curve decreased slightly, and the brittle failure behavior was not obvious. The reasons are as follows: As a two-dimensional nanomaterial with excellent mechanical properties, CNTs form a strong interfacial bond with the aerogel matrix skeleton through the condensation of hydroxyl groups, and form a strong composite structural framework.[28] On the one hand, this increases the bonding strength between secondary particles in the matrix, making it less prone to brittle failure.[21] On the other hand, when the brittle fracture of the aerogel matrix skeleton occurs, the CNTs can play a connecting role and effectively hinder the crack propagation, thereby inhibiting the progress of brittle failure of the composite.[20,54] Accordingly, as the CNTs content increased from 0 wt.% to 8 wt.%, the Young's modulus of the CNTs/silica aerogel composites increased from 410.4 kPa to 828.0 kPa (by 102%), and the compressive stress at 20% strain increased from 53.5 kPa to 127.6 kPa (by 139%), as given in Table 1. Furthermore, the Young's modulus of the composites increased significantly (by 95%) when the addition of CNTs ranged from 0 wt.% to 6 wt.%, while only showed an increase of ~4% as the CNTs content increased from 6% to 8% (Table 1). This is because the CNTs are difficult to be uniformly dispersed in silica sol by ultrasonic dispersion when their content is too high, and the agglomeration and sedimentation of CNTs have a negative impact on their strengthening effect. Notably, when the CNTs content reached 6 wt.%, the agglomeration and deposition phenomena are relatively mild and only have a small impact on the enhancement effect. However, when the CNTs content reached 8 wt.%, the obvious agglomeration and deposition phenomena significantly deteriorate the enhancement effect.

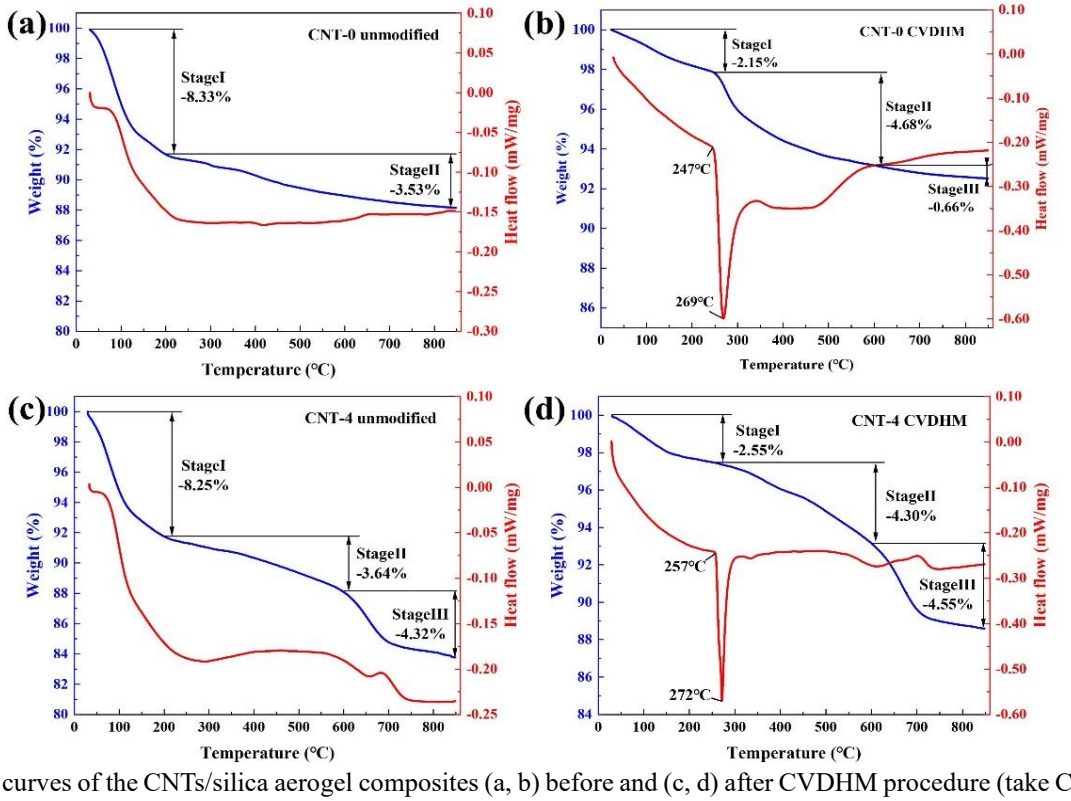

Fig. 9 TG-DSC curves of the CNTs/silica aerogel composites (a, b) before and (c, d) after CVDHM procedure (take CNT-0 and CNT-4 samples as examples).

Table 1. The detailed mechanical properties of the CNTs/silica aerogel composite samples CNT-0 to CNT-8, including the Young's modulus, σ10%, σ15%, and σ20%.

Samples	Young's modulus (kPa)	σ10% (kPa)	σ15% (kPa)	σ20% (kPa)
CNT-0	410.4 ± 11.1	39.0 ± 2.6	45.6 ± 6.4	53.5 ± 5.1
CNT-2	557.8 ± 8.6	49.4 ± 2.3	66.0 ± 3.9	86.2 ± 3.5
CNT-4	658.6 ± 7.5	55.9 ± 1.3	81.0 ± 2.4	105.5 ± 3.5
CNT-6	797.6 ± 20.6	64.7 ± 1.4	92.9 ± 1.8	117.8 ± 2.4
CNT-8	828.0 ± 24.7	72.9 ± 4.2	101.1 ± 5.5	127.6 ± 4.7

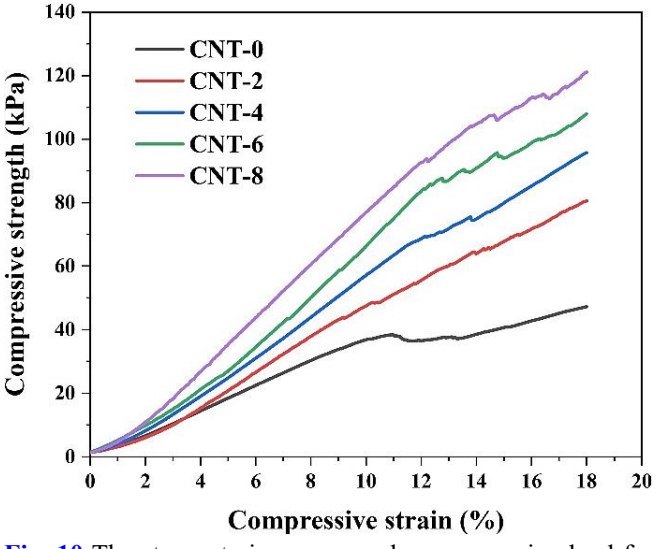

Fig. 10 The stress-strain curves under compressive load for the CNTs/silica aerogel composites CNT-0 to CNT-8.

4. Conclusion

In this work, we successfully prepared superhydrophobic high-quality monolithic carbon nanotubes (CNTs) reinforced silica aerogel composites using tert-butanol/water co-solvent as the freeze-drying solvent. The effects of CNTs on the pore structures, thermal performance and mechanical properties of the CNTs/silica aerogel composites were investigated. The main conclusions are summarized as follows:

(1) The freeze-drying process has caused no obvious damage to the nanoporous skeleton structure of the aerogel matrix.

(2) When the CNTs content is below 4 wt.%, the CNTs are uniformly distributed in the silica aerogel matrix and form a good interface combination with the aerogel skeleton. The pore structures and thermal conductivity of the composites were only slightly influenced, while the mechanical properties were greatly improved from 401.4 kPa to 658.6 kPa.

(3) When the CNTs content is above 6 wt.%, they began to agglomerate and entangle with each other in the matrix, which leads to the deterioration of pore structure and thermal insulation properties of the composite. When the content of CNTs reached 8 wt.%, its enhancing effect on mechanical properties has also significantly deteriorated.

(4) Due to the effective CVDHM process, the CNTs/silica aerogel composites show superhydrophobicity with a contact angle higher than 150°, which can maintain a thermal stability up to 257 °C.

Conflict of Interest

There is no conflict of interest.

Supporting Information

Not applicable.

References

[1] M.A. Aegerter, N. Leventis, M.M. Koebel, Aerogels Handbook, History of Aerogels, Chapter 1, 2011.

[2] A. Soleimani Dorcheh, M. H. Abbasi, Silica aerogel; synthesis, properties and characterization, *Journal of Materials Processing Technology*, 2008, **199**, 10-26, doi: 10.1016/j.jmatprotec.2007.10.060.

[3] L.-W. Hrubesh, L.-E. Keene, V.-R. Latorre, Dielectric properties of aerogels, *Journal of Materials Research*, 1993, **8**, 1736-1741, doi: 10.1557/JMR.1993.1736.

[4] H. Maleki, Recent advances in aerogels for environmental remediation applications: a review, *Chemical Engineering Journal*, 2016, **300**, 98-118, doi: 10.1016/j.cej.2016.04.098.

[5] S. M. Jones, Aerogel: space exploration applications, *Journal of Sol-Gel Science and Technology*, 2006, **40**, 351-357, doi: 10.1007/s10971-006-7762-7.

[6] Q. Fu, Y. Si, C. Duan, Z. Yan, L. Liu, J. Yu, B. Ding, Highly carboxylated, cellular structured, and underwater superelastic nanofibrous aerogels for efficient protein separation, *Advanced Functional Materials*, 2019, **29**, 1808234, doi: 10.1002/adfm.201808234.

[7] J. Martin, B. Hosticka, C. Lattimer, P. M. Norris, Mechanical and acoustical properties as a function of PEG concentration in macroporous silica gels, *Journal of Non-Crystalline Solids*, 2001, **285**, 222-229, doi: 10.1016/s0022-3093(01)00457-4.

[8] D. Bozoglu, H. Deligoz, K. Ulutas, S. Yakut, D. Deger, Structural and dielectrical characterization of low-k polyurethane composite films with silica aerogel, *Journal of Physics and Chemistry of Solids*, 2019, **130**, 46-57, doi: 10.1016/j.jpcs.2019.02.013.

[9] N. Leventis, C. Sotiriou-Leventis, G. Zhang, A.-M M. Rawashdeh, Nanoengineering strong silica aerogels, *Nano Letters*, 2002, **2**, 957-960, doi: 10.1021/nl025690e.

[10] N. de la Rosa-Fox, V. Morales-Flórez, J. A. Toledo-Fernández, M. Piñero, R. Mendoza-Serna, L. Esquivias, Nanoindentation on hybrid organic/inorganic silica aerogels, *Journal of the European Ceramic Society*, 2007, **27**, 3311-

3316, doi: 10.1016/j.jeurceramsoc.2007.02.209.
[11] S. Zhao, Z. Zhang, G. Sèbe, R. Wu, R. V. Rivera Virtudazo, P. Tingaut, M. M. Koebel, Multiscale assembly of superinsulating silica aerogels within silylated nanocellulosic scaffolds: improved mechanical properties promoted by nanoscale chemical compatibilization, *Advanced Functional Materials*, 2015, **25**, 2326-2334, doi: 10.1002/adfm.201404368.
[12] X. Tang, A. Sun, C. Chu, M. Yu, S. Ma, Y. Cheng, J. Guo, G. Xu, A novel silica nanowire-silica composite aerogels dried at ambient pressure, *Materials & Design*, 2017, **115**, 415-421, doi: 10.1016/j.matdes.2016.11.080.
[13] T. Matias, C. Varino, H. C. de Sousa, M. E. M. Braga, A. Portugal, J. F. J. Coelho, L. Durães, Novel flexible, hybrid aerogels with vinyl- and methyltrimethoxysilane in the underlying silica structure, *Journal of Materials Science*, 2016, **51**, 6781-6792, doi: 10.1007/s10853-016-9965-9.
[14] B. N. Nguyen, M. A. B. Meador, A. Medoro, V. Arendt, J. Randall, L. McCorkle, B. Shonkwiler, Elastic behavior of methyltrimethoxysilane based aerogels reinforced with tri-isocyanate, *ACS Applied Materials & Interfaces*, 2010, **2**, 1430-1443, doi: 10.1021/am100081a.
[15] Y. Si, X. Wang, L. Dou, J. Yu, B. Ding, Ultralight and fire-resistant ceramic nanofibrous aerogels with temperature-invariant superelasticity, *Science Advances*, 2018, **4**, eaas8925, doi: 10.1126/sciadv.aas8925.
[16] Y. Si, X. Wang, C. Yan, L. Yang, J. Yu, B. Ding, Ultralight biomass-derived carbonaceous nanofibrous aerogels with superelasticity and high pressure-sensitivity, *Advanced Materials*, 2016, **28**, 9512-9518, doi: 10.1002/adma.201603143.
[17] F. Wang, J. Dai, L. Huang, Y. Si, J. Yu, B. Ding, Biomimetic and superelastic silica nanofibrous aerogels with rechargeable bactericidal function for antifouling water disinfection, *ACS Nano*, 2020, **14**, 8975-8984, doi: 10.1021/acsnano.0c03793.
[18] S. Fu, Effects of fiber length and fiber orientation distributions on the tensile strength of short-fiber-reinforced polymers, *Composites Science and Technology*, 1996, **56**, 1179-1190, doi: 10.1016/s0266-3538(96)00072-3.
[19] J.-J. Zhao, Y.-Y. Duan, X.-D. Wang, B.-X. Wang, An analytical model for combined radiative and conductive heat transfer in fiber-loaded silica aerogels, *Journal of Non-Crystalline Solids*, 2012, **358**, 1303-1312, doi: 10.1016/j.jnoncrysol.2012.02.037.
[20] T. Linhares, M. T. Pessoa de Amorim, L. Durães, Silica aerogel composites with embedded fibres: a review on their preparation, properties and applications, *Journal of Materials Chemistry A*, 2019, **7**, 22768-22802, doi: 10.1039/c9ta04811a.
[21] A. Lamy-Mendes, R. F. Silva, L. Durães, Advances in carbon nanostructure–silica aerogel composites: a review, *Journal of Materials Chemistry A*, 2018, **6**, 1340-1369, doi: 10.1039/c7ta08959g.
[22] G. Zu, X. Wang, K. Kanamori, K. Nakanishi, Superhydrophobic highly flexible doubly cross-linked aerogel/carbon nanotube composites as strain/pressure sensors, *Journal of Materials Chemistry B*, 2020, **8**, 4883-4889, doi: 10.1039/c9tb02953b.
[23] A. I. Chernov, A. Y. Predein, A. F. Danilyuk, V. L. Kuznetsov, T. V. Larina, E. D. Obraztsova, Optical properties of silica aerogels with embedded multiwalled carbon nanotubes, *Physica Status Solidi (b)*, 2016, **253**, 2440-2445, doi: 10.1002/pssb.201600326.
[24] H. Bargozin, L. Amirkhani, J. S. Moghaddas, M. M. Ahadian, Synthesis and application of silica aerogel-MWCNT nanocomposites for adsorption of organic pollutants, *Scientia Iranica*, 2010, **17**, 122-132.
[25] X.-Y. Song, W. Cao, M. R. Ayers, A. J. Hunt, Carbon nanostructures in silica aerogel composites, *Journal of Materials Research*, 1995, **10**, 251-254, doi: 10.1557/JMR.1995.0251.
[26] J. G. Duque, C. E. Hamilton, G. Gupta, S. A. Crooker, J. J. Crochet, A. Mohite, H. Htoon, K. A. D. Obrey, A. M. Dattelbaum, S. K. Doorn, Fluorescent single-walled carbon nanotube aerogels in surfactant-free environments, *ACS Nano*, 2011, **5**, 6686-6694, doi: 10.1021/nn202225k.
[27] T. Sun, Q. Zhuo, X. Liu, Z. Sun, Z. Wu, H. Fan, Hydrophobic silica aerogel reinforced with carbon nanotube for oils removal, *Journal of Porous Materials*, 2014, **21**, 967-973, doi: 10.1007/s10934-014-9845-0.
[28] U. K. H. Bangi, M. S. Kavale, S. Baek, H.-H. Park, Synthesis of MWCNTs doped sodium silicate based aerogels by ambient pressure drying, *Journal of Sol-Gel Science and Technology*, 2012, **62**, 201-207, doi: 10.1007/s10971-012-2710-1.
[29] S. Yun, H. Luo, Y. Gao, Low-density, hydrophobic, highly flexible ambient-pressure-dried monolithic bridged silsesquioxane aerogels, *Journal of Materials Chemistry A*, 2015, **3**, 3390-3398, doi: 10.1039/c4ta05271d.
[30] J. Fu, S. Wang, C. He, Z. Lu, J. Huang, Z. Chen, Facilitated fabrication of high strength silica aerogels using cellulose nanofibrils as scaffold, *Carbohydrate Polymers*, 2016, **147**, 89-96, doi: 10.1016/j.carbpol.2016.03.048.
[31] K. Kraiwattanawong, H. Tamon, P. Praserthdam, Influence of solvent species used in solvent exchange for preparation of mesoporous carbon xerogels from resorcinol and formaldehyde via subcritical drying, *Microporous and Mesoporous Materials*, 2011, **138**, 8-16, doi: 10.1016/j.micromeso.2010.10.001.
[32] C. Jiménez-Saelices, B. Seantier, B. Cathala, Y. Grohens, Spray freeze-dried nanofibrillated cellulose aerogels with thermal superinsulating properties, *Carbohydrate Polymers*, 2017, **157**, 105-113, doi: 10.1016/j.carbpol.2016.09.068.
[33] Q. Shang, J. Chen, Y. Hu, X. Yang, L. Hu, C. Liu, X. Ren, Y. Zhou, Facile fabrication of superhydrophobic cross-linked nanocellulose aerogels for oil–water separation, *Polymers*, 2021, **13**, 625, doi: 10.3390/polym13040625.
[34] F. H. H. Abdellatif, M. M. Abdellatif, Bio-based i-carrageenan aerogels as efficient adsorbents for heavy metal ions and acid dye from aqueous solution, *Cellulose*, 2020, **27**,

441-453, doi: 10.1007/s10570-019-02818-x.
[35] D. K. Le, G. N. Ng, H. W. Koh, X. Zhang, Q. B. Thai, N. Phan-Thien, H. M. Duong, Methyltrimethoxysilane-coated recycled polyethylene terephthalate aerogels for oil spill cleaning applications, *Materials Chemistry and Physics*, 2020, **239**, 122064, doi: 10.1016/j.matchemphys.2019.122064.
[36] C. Wang, X. Chen, B. Wang, M. Huang, B. Wang, Y. Jiang, R. S. Ruoff, Freeze-casting produces a graphene oxide aerogel with a radial and centrosymmetric structure, *ACS Nano*, 2018, **12**, 5816-5825, doi: 10.1021/acsnano.8b01747.
[37] C. Li, J. Yang, P. Pachfule, S. Li, M.-Y. Ye, J. Schmidt, A. Thomas, Ultralight covalent organic framework/graphene aerogels with hierarchical porosity, *Nature Communications*, 2020, **11**, 4712, doi: 10.1038/s41467-020-18427-3.
[38] Y. Pan, S. He, L. Gong, X. Cheng, C. Li, Z. Li, Z. Liu, H. Zhang, Low thermal-conductivity and high thermal stable silica aerogel based on MTMS/Water-glass co-precursor prepared by freeze drying, *Materials & Design*, 2017, **113**, 246-253, doi: 10.1016/j.matdes.2016.09.083.
[39] A. Pons, L. Casas, E. Estop, E. Molins, K. D. M. Harris, M. Xu, A new route to aerogels: Monolithic silica cryogels, *Journal of Non-Crystalline Solids*, 2012, **358**, 461-469, doi: 10.1016/j.jnoncrysol.2011.10.031.
[40] A. C. Pierre, G. M. Pajonk, Chemistry of aerogels and their applications, *Chemical Reviews*, 2002, **102**, 4243-4266, doi: 10.1021/cr0101306.
[41] R. Daoussi, E. Bogdani, S. Vessot, J. Andrieu, O. Monnier, Freeze-drying of an active principle ingredient using organic co-solvent formulations: influence of freezing conditions and formulation on solvent crystals morphology, thermodynamics data, and sublimation kinetics, *Drying Technology*, 2011, **29**, 1858-1867, doi: 10.1080/07373937.2011.569624.
[42] H. Liu, P. Chu, H. Li, H. Zhang, J. Li, Novel three-dimensional halloysite nanotubes/silica composite aerogels with enhanced mechanical strength and low thermal conductivity prepared at ambient pressure, *Journal of Sol-Gel Science and Technology*, 2016, **80**, 651-659, doi: 10.1007/s10971-016-4154-5.
[43] S. Zong, W. Wei, Z. Jiang, Z. Yan, J. Zhu, J. Xie, Characterization and comparison of uniform hydrophilic/hydrophobic transparent silica aerogel beads: skeleton strength and surface modification, *RSC Advances*, 2015, **5**, 55579-55587, doi: 10.1039/c5ra08714g.
[44] A. V. Rao, P. B. Wagh, Preparation and characterization of hydrophobic silica aerogels, *Materials Chemistry and Physics*, 1998, **53**, 13-18, doi: 10.1016/s0254-0584(97)02047-6.
[45] Y. Lei, Z. Hu, B. Cao, X. Chen, H. Song, Enhancements of thermal insulation and mechanical property of silica aerogel monoliths by mixing graphene oxide, *Materials Chemistry and Physics*, 2017, **187**, 183-190, doi: 10.1016/j.matchemphys.2016.11.064.
[46] X. Li, Q. Wang, H. Li, H. Ji, X. Sun, J. He, Effect of sepiolite fiber on the structure and properties of the sepiolite/silica aerogel composite, *Journal of Sol-Gel Science and Technology*, 2013, **67**, 646-653, doi: 10.1007/s10971-013-3124-4.
[47] G. Lu, X.-D. Wang, Y.-Y. Duan, X.-W. Li, Effects of non-ideal structures and high temperatures on the insulation properties of aerogel-based composite materials, *Journal of Non-Crystalline Solids*, 2011, **357**, 3822-3829, doi: 10.1016/j.jnoncrysol.2011.07.022.
[48] T.-Y. Wei, S.-Y. Lu, Y.-C. Chang, A new class of opacified monolithic aerogels of ultralow high-temperature thermal conductivities, *The Journal of Physical Chemistry C*, 2009, **113**, 7424-7428, doi: 10.1021/jp900380q.
[49] Z. Li, L. Gong, X. Cheng, S. He, C. Li, H. Zhang, Flexible silica aerogel composites strengthened with aramid fibers and their thermal behavior, *Materials & Design*, 2016, **99**, 349-355, doi: 10.1016/j.matdes.2016.03.063.
[50] T. Zhou, X. Cheng, Y. Pan, C. Li, L. Gong, H. Zhang, Mechanical performance and thermal stability of glass fiber reinforced silica aerogel composites based on co-precursor method by freeze drying, *Applied Surface Science*, 2018, **437**, 321-328, doi: 10.1016/j.apsusc.2017.12.146.
[51] H. Liu, W. Sha, A. T. Cooper, M. Fan, Preparation and characterization of a novel silica aerogel as adsorbent for toxic organic compounds, *Colloids and Surfaces A: Physicochemical and Engineering Aspects*, 2009, **347**, 38-44, doi: 10.1016/j.colsurfa.2008.11.033.
[52] J. Li, Y. Lei, D. Xu, F. Liu, J. Li, A. Sun, J. Guo, G. Xu, Improved mechanical and thermal insulation properties of monolithic attapulgite nanofiber/silica aerogel composites dried at ambient pressure, *Journal of Sol-Gel Science and Technology*, 2017, **82**, 702-711, doi: 10.1007/s10971-017-4359-2.
[53] Y. Yang, E. Shi, P. Li, D. Wu, S. Wu, Y. Shang, W. Xu, A. Cao, Q. Yuan, A compressible mesoporous SiO_2 sponge supported by a carbon nanotube network, *Nanoscale*, 2014, **6**, 3585, doi: 10.1039/c3nr05931f.
[54] D. Shi, Y. Sun, J. Feng, X. Yang, S. Han, C. Mi, Y. Jiang, H. Qi, Experimental investigation on high temperature anisotropic compression properties of ceramic-fiber-reinforced SiO_2 aerogel, *Materials Science and Engineering: A*, 2013, **585**, 25-31, doi: 10.1016/j.msea.2013.07.029.

